On Matching Cross-Spectral Periocular Images for Accurate Biometrics Identification

N. Pattabhi Ramaiah, Ajay Kumar
Department of Computing, The Hong Kong Polytechnic University, Hong Kong
Email: n.p.in@ieee.org, ajaykr@ieee.org

Abstract

Periocular recognition has gained significant importance with the increasing use of surgical masks to safeguard against environmental pollution or for improving accuracy of iris recognition. This paper proposes a new framework for accurately matching cross-spectral periocular images using Markov random fields (MRF) and three patch local binary patterns (TPLBP). We study the problem of cross-spectral periocular recognition from a new perspective and our study indicates that such recognition can be considerably improved if we can preserve pixel correspondences among two matched images. The matching accuracy for cross-spectral periocular matching can be further improved by incorporating real-valued features that can be simultaneously recovered from pixels in the iris regions. We present experimental results from IIITD IMP database and PolyU database. Our experimental results validate the usefulness of this approach and achieve state-of-the-art performance for accurate cross-spectral periocular recognition.

1. Introduction

The periocular recognition [1] incorporates the surrounding information of an eye for the personal identification. This region is automatically acquired during the iris or face recognition imaging and especially suitable for identification when face region is largely covered from surgical masks or when face is covered to safe-guard against environmental pollution (see Fig. 1). Iris recognition [2, 3] is highly reliable, accurate and scalable for person identification when compared to other biometric technologies. Most of the facial recognition systems in surveillance applications use visible wavelengths to acquire the images whereas the iris images are generally acquired under near infrared illumination. In this context, the visible periocular images extracted from facial images should be matched with the periocular images acquired under near infra-red wavelengths. However accurately matching cross-spectral periocular regions is very challenging problem. Our observations from section 4 suggests serious degradation in matching accuracy over same spectrum images.

In this paper, we propose a framework to improve the cross-spectral matching accuracy using a variant of local binary patterns for extracting periocular features and by synthesizing near infrared to visible images using Markov random fields (MRF) model.

(a) (b)

Figure 1. Periocular recognition is often the only means to identify subjects with (a) surgical masks, (b) covered faces to safeguard against environmental pollution

This paper investigates the problem of cross-spectral periocular recognition using bi-spectral imaging. Such imaging can provide exact pixel correspondences between the near-infrared and visible spectrum pixels. Even though it is very challenging to address the problem cross-spectral periocular matching [4], the experimental results in this paper illustrate that the performance from the cross-spectral periocular recognition can significantly improve with the availability of pixel correspondences in such bi-spectral images. Secondly, this paper investigates a more accurate approach to match cross-spectral periocular images using three patch local binary patterns. The periocular information is further combined with simultaneously recovered iris region pixels which typically provide more information [5]. The key idea here is to synthesize the corresponding near infrared pixels from the visible[1] periocular images. These synthesized images can be matched with near infrared images to achieve cross-spectral matching. Our experimental results on PolyU dataset acquired from 209 different classes illustrate outperforming results. Our experimental results in section 4 also suggest that the performance for such cross-spectral periocular matching can be further improved by combining the match scores from simultaneously available iris images.

[1]The periocular images under visible imaging can be conveniently acquired during the surveillance

1.1. Related Work

Several researchers have explained [6] the importance of periocular recognition when iris recognition performance degrades under long distance and visible spectrum imaging. Juefei-Xu et al. [7] used the periocular information to improve the performance of age invariant face recognition. Some researchers [8, 9] illustrated a significant improvement in iris recognition performance when combining the periocular features with iris features. Periocular probabilistic deformation models (PPDMs) are proposed by considering the image deformation information for the periocular image verification in [10]. Image set classification problem [11] is formulated for the first time in periocular biometric recognition.

In the cross-spectral periocular recognition [12], the images acquired under visible wavelengths are matched against the images acquired under near infra-red wavelengths. There have been recent efforts to develop cross-spectral periocular as well as iris recognition systems. The selection of best regions for periocular images are introduced using cross spectral images in [13]. The fusion of periocular and iris recognition using cross-spectral images is presented in [14]. Reference [4] investigates cross-spectral periocular recognition using neural networks for learning the gap among different spectrum, namely, visible, night vision and near infrared. Reference [15] describes a framework for accurately segmenting the iris images from face images acquired at-a-distance under near infra-red or visible illuminations. Very few efforts have been made to analyze the multi-spectral iris imaging. Ross et al. [16] proposed the enhanced iris recognition system by considering the fusion of multiple spectrum beyond the wavelengths of $900nm$. An approach for cross spectral iris matching [17] was proposed using the predictive NIR image. A learning based approach for low-level vision problem is introduced in [18] for scene estimation from the images. In [19], an image synthesis method is proposed for the face photo-sketch recognition. A survey of prior work in cross-spectral periocular matching suggests that such matching performance is far below expectations for the deployment and need for further work in this area.

The rest of the paper is organized as follows: Section 2, describes our solution for cross-spectral iris recognition. The proposed model is evaluated on bi-spectral iris data (PolyU) in section 4. Finally, key conclusions from this paper are summerized in section 5.

2. Near Infrared to Visible Image Synthesis

We firstly define the notations used in this paper and then introduce the approach of near infrared to visible image data synthesis. Let Δ_i be the set of local image patches extracted from the normalized image i having width w and height h.

$$\Delta_i = \{\delta_{i_1}, \delta_{i_2}, ..., \delta_{i_P}\},\ \forall \delta_{i_p} \in \mathbb{R}^{d \times 2d} \tag{1}$$

where $p = \{1, 2, ...P\}$ and $d \times 2d$ is the size of local patch.

During image acquisition, all images from near infrared and visible wavelengths are aligned in a way that the spatial positions of the corresponding pixels of all images are similar. The normalized image region is divided into blocks with overlapping neighboring patches. For each patch along the input near infrared normalized image, the patch is estimated in the corresponding visible normalized image. In order to estimate the visible image patch δ_j^{vis} of the input near infrared image patch δ_j^{nir}; K, candidate visible normalized image patches $\left\{\bar{\delta_j^{vis}}^l\right\}_{l=1}^{K}$ are gathered from the training set. The synthesized visible image should meticulously match the input near infrared image in form and be smooth in the meanwhile. With a specific end goal to achieve this objective, a Markov network is utilized to model the process of visible texture synthesis.

Fig. 2 depicts the basic block diagram of the proposed NIR to VIS texture synthesis methodology developed in this work. Cross-spectral data is employed as input to the framework. Algorithm in [20] is being used for image segmentation, normalization and template extraction for the bi-spectral images. In order to segment the image ROI, the segmentation parameters of the NIR image are also employed for visible (R-channel) image segmentation. We introduce real-valued local feature descriptor which are obtained from phase angles obtained during spatial filtering. For cross-spectral iris recognition, texture synthesis (NIR to VIS) method is employed to enhance the matching performance.

2.1. Markov Random Fields (MRF) model

The graphical model of Markov network for our problem is illustrated in Fig.3 and can be constructed from the properties of low-level vision problems [18, 19, 21] which can be solved in two key phases, namely, $learning$ and $inference$. In $learning$ phase, the network parameters will be trained till it reaches optimnal solution, whereas the visible image patches are estimated in $inference$ phase.

The joint probability over visible (Δ^{vis}) and near infrared (Δ^{nir}) iris image patches for a Markov random field can be defined as follows:

$$\begin{aligned} &P(\Delta^{vis}, \Delta^{nir}) \\ &= P(\delta_1^{vis}, \delta_2^{vis}, ..., \delta_N^{vis}, \delta_1^{nir}, \delta_2^{nir}, ..., \delta_N^{nir}) \\ &= \prod_{(i,j)} \Gamma(\delta_i^{vis}, \delta_j^{vis}) \prod_k \vartheta(x_k, \delta_k^{nir}) \end{aligned} \tag{2}$$

where δ_i^{vis} has K possible states which are determined from the candidate visible image patches. The compatibility

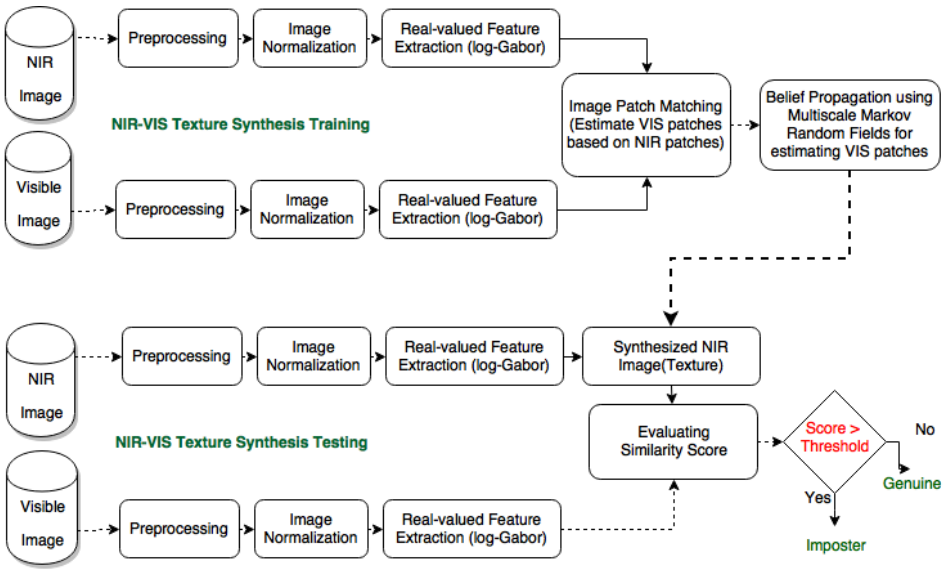

Figure 2. Block-diagram of the proposed Markov random fields (MRF) model for cross-spectral periocular recognition

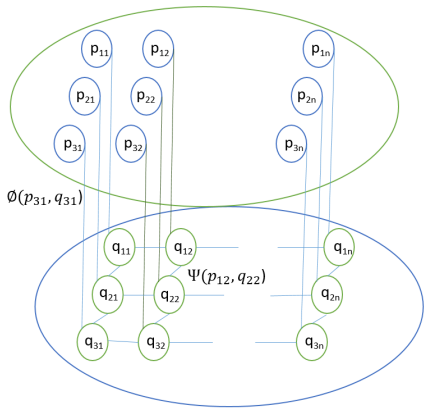

Figure 3. Markov network for infra-red and visible image patches where $\delta^{nir} = q_{ij}$ and $\delta^{vis} = p_{ij}$, p_{ij} means the i^{th} row and j^{th} column of visible image patches and q_{ij} means the i^{th} row and j^{th} column of near infra-red image patches.

function between visible image patches can be calculated as,

$$\Gamma(\delta_k^{vis.l}, \delta_j^{vis.m}) = e^{-|d_{jk}^l - d_{kj}^m|^2/2\sigma_{vis}^2} \quad (3)$$

where k and j are two neighboring visible image patches with a region of overlapping and d_{jk}^l, d_{kj}^m represent the intensity values of the overlapping region between the l^{th} and m^{th} candidate visible image patches. σ_{vis} is the Gaussian noise of covariance used to differ training data of visible images from the $ideal$ training data.

The local evidence can be calculated as follows:

$$\vartheta(\delta_k^{vis.l}, \delta_k^{nir}) = e^{-|\delta_k^{nir.l} - \delta_k^{nir}|^2/2\sigma_{nir}^2} \quad (4)$$

σ_{nir} is the Gaussian noise of covariance used to differ training data of near infra-red images from the $ideal$ training data and $\delta_k^{vis.l}$ represent l^{th} candidate visible image patch.

In the $learning$ phase of Markov network, the parameters will be computed by solving the following problem:

$$\hat{\delta^{vis}}_{j\ MAP} = \underset{\delta_j^{vis}}{\operatorname{argmax}} \max_{all\ \delta_i^{vis}, i \neq j} P(\delta_1^{vis}, \delta_2^{vis}, ..., \delta_N^{vis}, \delta_1^{nir}, \delta_2^{nir}, ..., \delta_N^{nir}) \quad (5)$$

where $\hat{\delta^{vis}}_{j\ MAP}$ is the MAP estimate for calculating maximum of marginal probabilities of all visible image patches.

In the $inference$ phase, belief propagation [21] is used for reaching network optimal solution. It passes the local $messages$ between the neighboring patches (or network nodes) in order to calculate the MAP estimate. The MAP estimate for visible image patch can be re-written as follows:

$$\hat{\delta^{vis}}_{j\ MAP} = \underset{\delta_j^{vis}}{\operatorname{argmax}}\, \vartheta(\delta_j^{vis}, \delta_j^{nir}) \prod_k M_j^k \quad (6)$$

Belief in patch j, is defined as the product of all local evidences of visible image patches and the messages entering into that visible image patch j. The message passes from node k to j can be represented as follows:

$$M_j^k = \max_{[\delta_k^{vis}]} \Gamma(\delta_j^{vis}, \delta_k^{vis}) \vartheta(\delta_k^{vis}, \delta_k^{nir}) \prod_{l \neq j} \hat{M}_k^l \quad (7)$$

The propagation rules in (7) are employed to achieve the optimal solution for Markov random fields. The network is trained using (5) and the updated unknown parameters are employed to synthesize visible spectrum patches from near infrared image patches for cross-spectral matching.

3. Matching ROI from Iris

The performance of periocular recognition is much better when compared to iris recognition for matching images acquired in two different wavelength spectrum (near infrared and visible). In the cross-domain imaging, the huge wavelength variations between the near infrared and visible spectrum suppress the discriminative power of minute details (iris texture) with minimal affect on ocular regions. However, cross-spectral iris recognition can further improve the performance of cross-spectral periocular recognition especially in the surveillance environment. As part of the feature extraction from periocular images, a variant of local binary patterns along with a new similarity measure based on real-valued representation of 1D log-Gabor filter responses is implemented. This real-valued features performs almost same as those using popular binarized iris codes for same sensor iris data, but unlike binary codes these features can be more appropriate for training Markov Random Fields (MRF) model. The frequency response of 1D log-Gabor filter can be defined as follows:

$$G(x) = e^{-\frac{1}{2}(log(\frac{x}{x_0})/(log(\frac{\sigma}{x_0}))^2} \quad (8)$$

where x_0, σ are the centre frequency and bandwidth of the filter, respectively. The 1D log-Gabor filter is convolved with each row of normalized iris image (i) which generates the complex response $(u + jv)$ for each pixel in i. The real (u) and imaginary (v) values of the complex number is typically quantized into either 0 or 1 based on sign of the response values. However, in our approach this complex value is converted into real value as follows:

$$u + jv \iff sgn(u) * 2 + sgn(v) \quad (9)$$

where $sgn(.)$ operator generates either 1 (if value is positive) or 0 (if value is negative). The feature descriptor is constructed using such real values and considered column-wise to form a vector of size, $h \times 1$.

4. Experiments and Results

In this section, we firstly describe the databases employed for the experiments to validate the approach detailed in section 2 for cross-spectral periocular matching.

4.1. PolyU Cross-Spectral Iris Database

The experiments were performed using the PolyU cross-spectral iris database. The database consists of total 12,550 iris images (209 $\times$ 2 $\times$ 2 $\times$ 15) which are acquired from 209 subjects of both eyes simultaneously in both near infra-red and visible channels each image in 15 different instances. The sample iris images acquired both in near-infrared and visible wavelengths are illustrated as shown in Fig. 4.

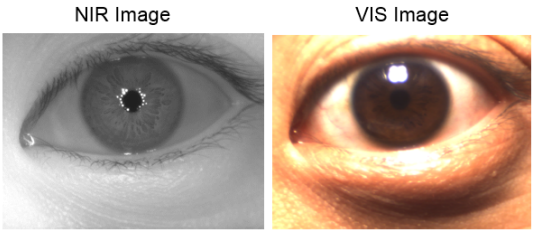

Figure 4. Sample bi-spectral iris images (PolyU database) simultaneously acquired under near infra-red and visible wavelengths

4.2. IIITD IMP database

The periocular recognition experiments were also performed on IIITD multi-spectral periocular database [4]. The database consists of total 1860 periocular images (62 $\times$ 2 $\times$ 3 $\times$ 5) which are acquired in 5 instances from 62 subjects of both eyes in near infra-red, night vision and visible channels. The sample periocular images are illustrated as shown in Fig. 5.

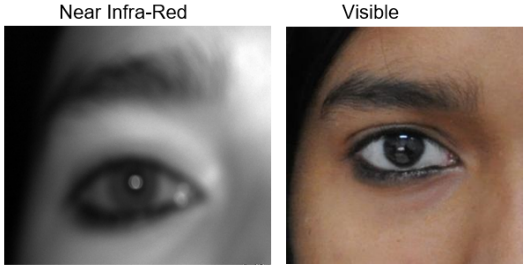

Figure 5. Sample multi-spectral periocular images (IMP)

4.3. Cross-Spectral Periocular Recognition

The experiments for cross-spectral periocular recognition were performed using IMP [4] and PolyU databases. Two variants of local binary patterns (LBP), namely, FPLBP (Four-Patch LBP) and TPLBP (Three-Patch LBP) methods [22] are employed on both databases with same protocol of comparisons. This generated 5,600 genuine and 1,953,000 imposter scores. From Table 1, it is observed the periocular recognition performance (GAR at 0.1 FAR) achieved at 73.2% on PolyU database, whereas it is 18.35% on IMP database. This difference can be attributed to the fact that only PolyU database has the exact pixel correspondences in both visible and near infra-red images. It can also be observed that TPLBP achieves significantly superior performance than FPLBP suggested in ref [4]. The corresponding receiver operating characteristic (ROC) curves are shown in Fig. 6(a).

Table 1. Genuine acceptance rate at 0.1 FAR for cross-spectral periocular recognition on IMP and PolyU databases

	FPLBP (IMP)	TPLBP (IMP)	FPLBP (PolyU)	TPLBP (PolyU)
NIR-VIS	15.93	18.35	45.4	73.2

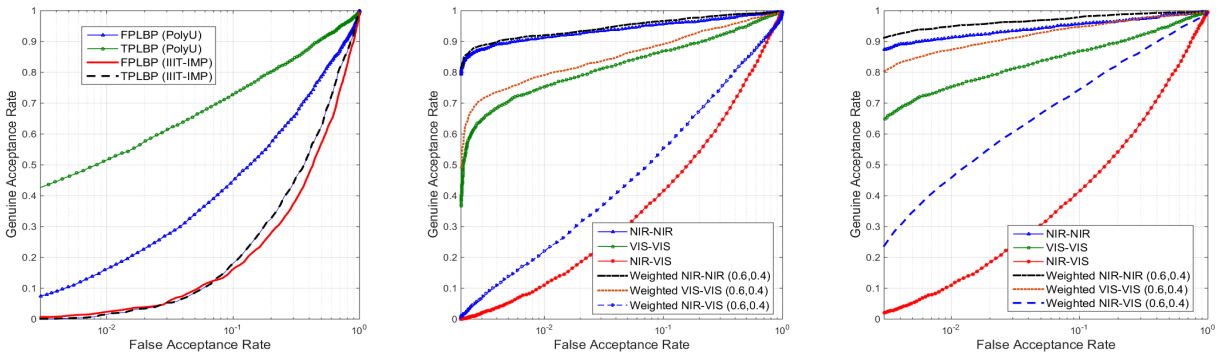

(a) (b) (c)

Figure 6. The ROC curve for cross-spectral periocular recognition using FPLBP and TPLBP on PolyU and IMP databases in (a), cross-spectral matching (LG+FPLBP) in (b), cross-spectral matching (LG+TPLBP) in (c).

4.3.1 Cross-Spectral Iris Recognition

This experiment were performed on 280 different classes of iris images (8,400 total images) are properly segmented in both visible and near infrared channels. The matching accuracy for the cross-spectral iris matching is ascertained from the equal error rate (EER) and ROC. The total number of genuine and imposter comparisons are 5,600 and 1,953,000, respectively. It is observed that even though the cross comparisons in near infra-red and visible channels are independently quite accurate, the performance of cross-spectral iris matching has significantly degraded. The EER for near infrared iris comparisons is 5.1% and for visible iris comparisons is 12.2%, whereas, for cross-spectral iris comparisons, it is observed that the EER increases to 33.3%.

The results from the combinations of LG and TPLBP methods are shown in Fig. 6(c). The corresponding EERs from the ROCs in Fig. 6(b) and Fig. 6(c) are comparatively presented in Table 2 where N-N, V-V and N-V mean NIR-NIR, VIS-VIS and NIR-VIS comparisons, respectively. The EER for the best performing cross-spectral periocular and iris matching is observed to be 17.9% which results from the combination of TPLBP and log-Gabor filter. The corresponding recognition performance rate is achieved at 74.7%. The weighted fusion can be computed as, $w_{NIR} * Score_{NIR} + (1 - w_{NIR}) * Score_{VIS}$. Our experimental results in Fig. 6 suggest that the combination of periocular and iris recognition results can offer significant performance improvement for the cross-spectral iris recognition.

4.3.2 Cross-Spectral Iris Recognition using MRF

The MRF based approach detailed in section 2.1 can be employed to achieve more accurate cross-spectral iris recognition performance. The ROC curves for such cross-spectral iris recognition performance on PolyU database are shown in Fig. 7. These results demonstrate that there is significant improvement in the cross-spectral iris recognition performance, (61.9%) over the conventional iris code approach (41.8%). The matching performance can be further im-

Table 2. EERs from the same- & cross-spectral matching (LG represents iris matching using 1-D log-Gobor filter while FPLBP and TPLBP represents respective methods for periocular matching)

	LG	FPLBP	LG + FPLBP	TPLBP	LG + TPLBP
N-N	5.1	26.1	4.4	10.9	3.1
V-V	12.1	26.2	10.3	11.5	6.1
N-V	33.4	32.5	26.6	19.8	17.9

Table 3. Genuine acceptance rate at 0.1 % FAR for various cross-spectral combinations

	LG	MRF	LG + TPLBP	LG + TPLBP + MRF
NIR-VIS	41.8	61.9	74.7	84.2

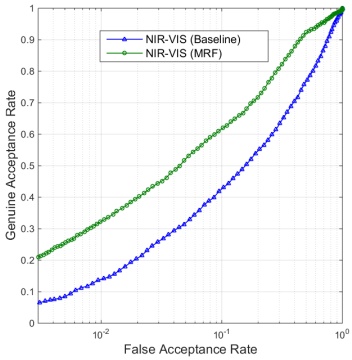

Figure 7. The ROC curve for cross-spectral iris recognition using MRF model

proved to 84.2% when MRF results are further combined with LG and TPLBP results using score level fusion.

5. Conclusions

This paper has developed a new framework for cross-spectral periocular recognition, particularly for matching iris images with exact pixel-to-pixel correspondences. It uses a variant of local binary patterns (LBP) for periocular feature extraction and Markov random fields (MRF) model for synthesizing visible iris data patches from the trained near infrared iris data patches. The experimental results presented in this paper on PolyU bi-spectral imaging illustrate significant improvement in periocular recognition performance over prior methods in the literature.

6. Acknowledgements

This work is supported by general research fund from the Research Grant Council of Hong Kong, grant number PolyU 152068/14E. Authors would like to thank IIIT Delhi for providing the multi-spectral periocular image database.

References

[1] U. Park, R. Jillela, A. Ross, and A. K. Jain, "Periocular biometrics in the visible spectrum," *Information Forensics and Security, IEEE Transactions on*, vol. 6, no. 1, pp. 96–106, 2011.

[2] M. J. Burge and K. W. Bowyer, *Handbook of Iris Recognition*. Springer-Verlag London, 2013.

[3] J. G. Daugman, "High confidence visual recognition of persons by a test of statistical independence," *Pattern Analysis and Machine Intelligence, IEEE Transactions on*, vol. 15, no. 11, pp. 1148–1161, 1993.

[4] A. Sharma, S. Verma, M. Vatsa, and R. Singh, "On cross spectral periocular recognition," in *Image Processing (ICIP), 2014 IEEE International Conference on*. IEEE, 2014, pp. 5007–5011.

[5] N. P. Ramaiah and A. Kumar, "Towards more accurate iris recognition using bi-spectral imaging and cross-spectral matching capability," *Technical Report No. COMP-K-21*, Dec. 2015.

[6] S. Bharadwaj, H. S. Bhatt, M. Vatsa, and R. Singh, "Periocular biometrics: When iris recognition fails," in *Biometrics: Theory Applications and Systems (BTAS), 2010 Fourth IEEE International Conference on*. IEEE, 2010, pp. 1–6.

[7] F. Juefei-Xu, K. Luu, M. Savvides, T. D. Bui, and C. Y. Suen, "Investigating age invariant face recognition based on periocular biometrics," in *Biometrics (IJCB), 2011 International Joint Conference on*. IEEE, 2011, pp. 1–7.

[8] C.-W. Tan and A. Kumar, "Towards online iris and periocular recognition under relaxed imaging constraints," *Image Processing, IEEE Transactions on*, vol. 22, no. 10, pp. 3751–3765, 2013.

[9] D. L. Woodard, S. Pundlik, P. Miller, R. Jillela, and A. Ross, "On the fusion of periocular and iris biometrics in non-ideal imagery," in *Pattern Recognition (ICPR), 2010 20th International Conference on*. IEEE, 2010, pp. 201–204.

[10] J. M. Smereka, V. N. Boddeti, and B. Vijaya Kumar, "Probabilistic deformation models for challenging periocular image verification," *Information Forensics and Security, IEEE Transactions on*, vol. 10, no. 9, pp. 1875–1890, 2015.

[11] M. Uzair, A. Mahmood, A. Mian, and C. McDonald, "Periocular biometric recognition using image sets," in *Applications of Computer Vision (WACV), 2013 IEEE Workshop on*. IEEE, 2013, pp. 246–251.

[12] K. P. Hollingsworth, S. S. Darnell, P. E. Miller, D. L. Woodard, K. W. Bowyer, and P. J. Flynn, "Human and machine performance on periocular biometrics under near-infrared light and visible light," *Information Forensics and Security, IEEE Transactions on*, vol. 7, no. 2, pp. 588–601, 2012.

[13] F. Alonso-Fernandez and J. Bigun, "Best regions for periocular recognition with nir and visible images," in *Image Processing (ICIP), 2014 IEEE International Conference on*. IEEE, 2014, pp. 4987–4991.

[14] F. Alonso-Fernandez, A. Mikaelyan, and J. Bigun, "Comparison and fusion of multiple iris and periocular matchers using near-infrared and visible images," in *Biometrics and Forensics (IWBF), International Workshop on*, 2015, pp. 1–6.

[15] C.-W. Tan and A. Kumar, "Unified framework for automated iris segmentation using distantly acquired face images," *Image Processing, IEEE Transactions on*, vol. 21, no. 9, pp. 4068–4079, 2012.

[16] A. Ross, R. Pasula, and L. Hornak, "Exploring multispectral iris recognition beyond 900nm," in *Biometrics: Theory, Applications, and Systems, 2009. BTAS'09. IEEE 3rd International Conference on*. IEEE, 2009, pp. 1–8.

[17] J. Zuo, F. Nicolo, and N. A. Schmid, "Cross spectral iris matching based on predictive image mapping," in *Biometrics: Theory Applications and Systems (BTAS), 2010 Fourth IEEE International Conference on*. IEEE, 2010, pp. 1–5.

[18] W. T. Freeman, E. C. Pasztor, and O. T. Carmichael, "Learning low-level vision," *International Journal of Computer Vision*, vol. 40, no. 1, pp. 25–47, 2000.

[19] X. Wang and X. Tang, "Face photo-sketch synthesis and recognition," *Pattern Analysis and Machine Intelligence, IEEE Transactions on*, vol. 31, no. 11, pp. 1955–1967, 2009.

[20] L. Masek and P. Kovesi, "Matlab source code for a biometric identification system based on iris patterns," *The School of Computer Science and Software Engineering, The University of Western Australia*, vol. 2, no. 4, 2003.

[21] J. S. Yedidia, W. T. Freeman, and Y. Weiss, "Understanding belief propagation and its generalizations," *Exploring Artificial Intelligence in the New Millennium*, vol. 8, pp. 236–239, Morgan Kaufmann Publishers Inc., 2003.

[22] L. Wolf, T. Hassner, and Y. Taigman, "Descriptor based methods in the wild," in *Workshop on Faces in'Real-Life'Images: Detection, Alignment, and Recognition*, 2008.